

Fig. 5.18: Detail of the Matlab/Simulink model

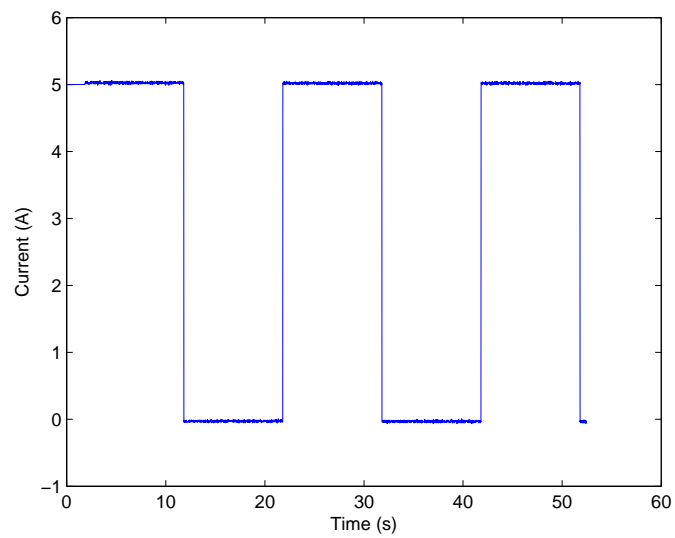


Fig. 5.19: Discharge current profile required to the battery

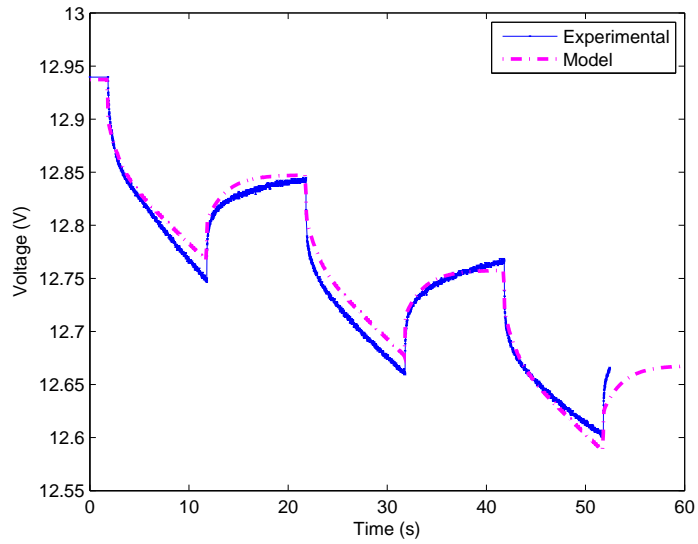


Fig. 5.20: Experimental and modeled battery voltage during discharge

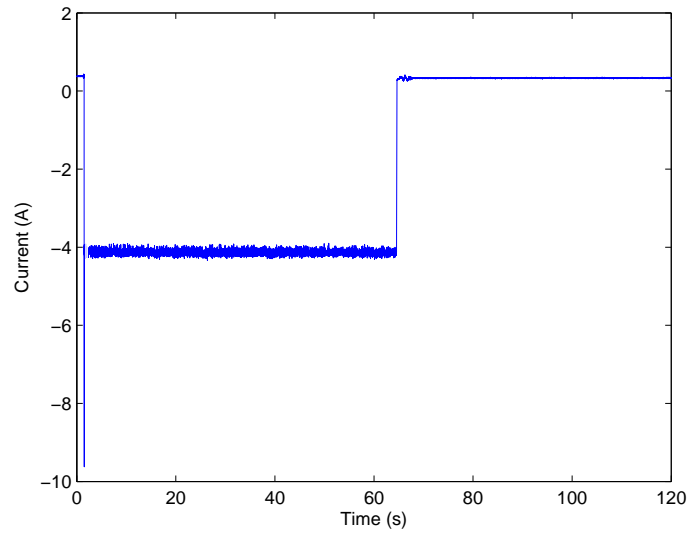


Fig. 5.21: Charge current profile injected in the battery

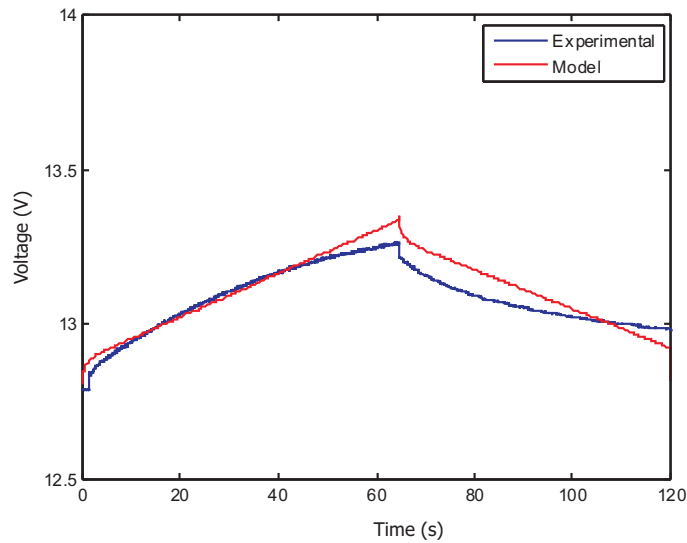


Fig. 5.22: Experimental and modeled battery voltage during charge

and power (W), i.e. in absolute magnitudes. This approach corresponds to the basic way power engineers solve electrical circuits and power systems.

But this classic approach needs to be changed when energy storage systems, such as batteries are incorporated to a power system. With this classic point of view, the general assumption is that the energy delivered by the power sources is unlimited. This may be true for other power sources, but not for batteries or other energy storage system. Apart from voltage, current, power and impedance storage systems are not completely defined without an additional variable: the available energy stored and ready to be delivered at a given instant.

For the analysis of power systems which present different voltage levels, the usual way to describe the variables is in per-unit values (p.u.) relative to a defined set of base values. The usual set of variables are power, voltage, current and impedance. However, when energy comes into play a new base magnitude needs to be included: the base time. Time is taken into account in the variable "battery capacity", expressed in Amperes hour (A·h), which is the product of the rated current times the rated discharge time. Therefore, the classic base magnitudes have to be revised and new magnitudes included.

Author	Voltage (V)	Capacity (A·h)	<i>Rohm</i> (mΩ)
Blanke [72]	12	70	5.2
Gauchia	12	50	3.2
Hariprakash [71]	6	4	75
Karden [88]	4	100	0.6
Salkind [15]	12	100	6.5
Salkind [15]	6	10	5

Table 5.4: Comparison between different authors

Curiously, there is a mixture of per-unit and absolute variables which have been used by both electrochemical and power engineers. For example, voltage is expressed in V, current in A, but battery state of charge is defined as a percentage, that is, a dimensionless variable. In most cases, for electrochemical systems, power engineers inherit the vocabulary established by electrochemical engineers, even if an obvious different focus is given, but no in depth transformation has been done to adapt the inherited variables to the power engineering world. Furthermore, the current situation collides with the usual way power engineers use to represent and analyze the electrical power system.

The drawbacks of this mixed per-unit and absolute variables are clearly exposed when a comparison between the performance of batteries with different characteristics, or a sizing calculation is carried out. The variables, such as voltage, capacity, impedance, power, etc. can assume a wide range of values as they are dependant on the overall size of the system, defined by its rated capacity, voltage or current. For example, if one of the parameters of the equivalent circuit calculated previously is compared to those obtained by other authors, no clear conclusion about the correctness of the results can be concluded. Table 5.4 presents the results for the ohmic resistance at 70 % obtained by several authors.

Analyzing Table 5.4, no clear relationship can be extracted, as batteries with similar voltages and capacities exhibit very different impedances. Therefore, how can any author compare its results to those obtained by other authors?

This Thesis proposes the application of a per-unit system to batteries to

overcome these problems, explaining the need to use two different base times, in order to represent phenomena which occur in different time horizons, as it is the case of the long-term charge/discharge processes versus the transient phenomena. To this end, an equivalent circuit for a battery will be developed and its parameters will be calculated and represented as per-unit values. Finally, the proposed methodology will be applied to different cases referred in the bibliography and compared with experimental results obtained for this work.

5.6.1. Steady-state per-unit system for a battery

For energy storage devices such as batteries, the usual base variables used (voltage, current, power and impedance) is inadequate, as a base value for the energy stored or released by the battery must be defined. Hence, it is essential to introduce the concept of capacity, which is related with the discharge duration according to the Peukert equation [62].

$$C \cdot I^{pc-1} = constant \quad (5.5)$$

Where C is the rated capacity, I the current and pc the Peukert coefficient (usually between 0.5 and 2), which is unique for each technology and model. The equation reveals that the available capacity at constant discharge current is reduced for increasing discharge rates.

Therefore, a new set of base magnitude which includes a base capacity C_b related to a discharge time t_b must be created. Known the base capacity and the discharge time (information which can be easily found in the data sheet handed by the manufacturer), the base current can be obtained.

$$I_b(A) = \frac{C_b}{t_b} \quad (5.6)$$

If the "natural" choice of taking the open circuit voltage as base voltage is adopted, the rest of base values can be obtained, completing the set of base values necessary to describe the battery performance for stationary operation. All the base values are presented in Table 5.5. Evidently, if three values are suitably selected, the rest of the base values can be calculated. However, the selection criterion of the first three base values is not arbitrary as the base

Base capacity	Base discharge time	Base current	Base voltage	Base power	Base impedance
C_b (A·h)	t_b (h)	I_b (A)	U_b (V)	P_b (W)	Z_b (Ω)

Table 5.5: Proposed base variables for a battery

Author	U (V)	C (Ah)	t (h)	R (m Ω)	I _b (A)	Z _b (Ω)	R (p.u.)
Blanke	12	44	20	5,2	2,2	5,45	0,95
Gauchia	12	50	20	3,2	2,5	4,8	0,67
Hariprakash	6	4	5	75	0,8	7,5	10
Karden	4	100	10	0,6	10	0,4	0,24
Salkind	12	100	20	6,5	5	2,4	2,7
Salkind	6	10	20	5	0,5	12	0,42

Table 5.6: Proposed base variables for a battery

values must be linearly independent.

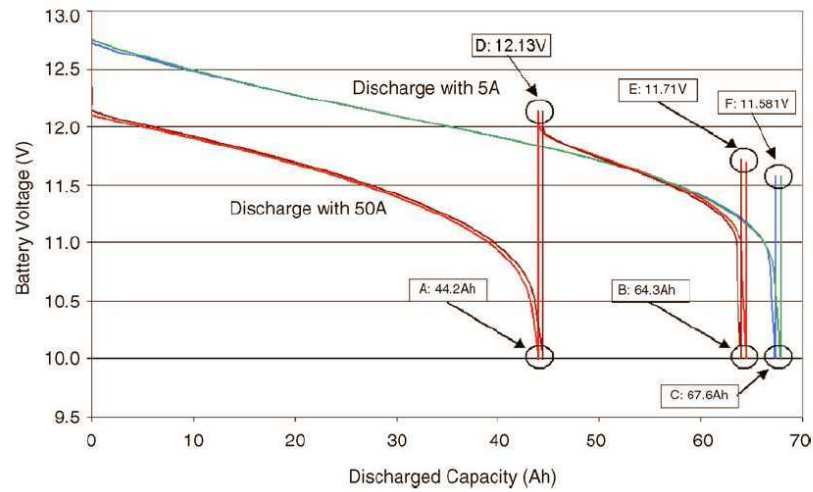
$$P_b = U_b \cdot I_b \quad Z_B = \frac{U_b}{I_b} \quad (5.7)$$

Table 5.6 completes Table 5.4 by adding the base magnitudes and by expressing the resistances in p.u. values. The base current is calculated known the discharge time for which the capacity is defined. The base impedance can be calculated as the ratio of the base voltage (rated value) and base current.

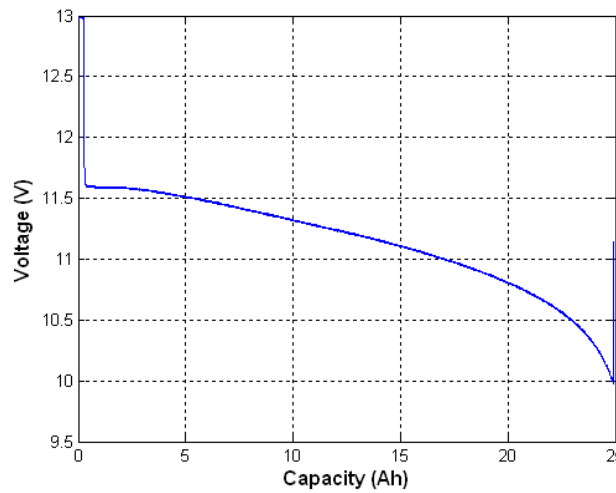
The comparison between the resistance values in absolute and per-unit values yields different information about the relationship between them. For example, the resistance obtained by Karden is one order of magnitude smaller than the one presented by Blanke or the obtained in this Thesis. No linear relationship can be found with voltage or capacity, which was also pointed out by Karden [88]. However, the three mentioned values are near enough when compared as p.u. values. Therefore, the comparison between absolute values can be misleading, as the capacity of the batteries influences, for example, the impedance.

5.6.2. Per unit representation of the discharge curve

The discharge curve is an extended representation of the evolution of the battery voltage with the discharged capacity. Its frequent use makes it ad-



a)



b)

Fig. 5.23: Discharge curve obtained by a)Doerffel and b)Gauchia in absolute values

visible to define it in per-unit values, in order to allow a direct comparison between curves obtained for different batteries, which can proceed from different manufacturers or can be from different technologies.

Fig. 5.23 a, taken from Doerffel [63] represents experimental results in which a battery apparently discharged at high discharge rate can be further discharged at a lower discharge rate, all variables being expressed in absolute values in the original work. Fig. 5.23 b represents a discharge curve obtained for the Exide-Tudor battery used in this Thesis.

Base capacity	Base discharge time	Base current	Base voltage	Base power	Base impedance
45 A·h	5 h	9 A	12 V	108 W	1.33 Ω

Table 5.7: Base values for the Exide-Tudor battery studied

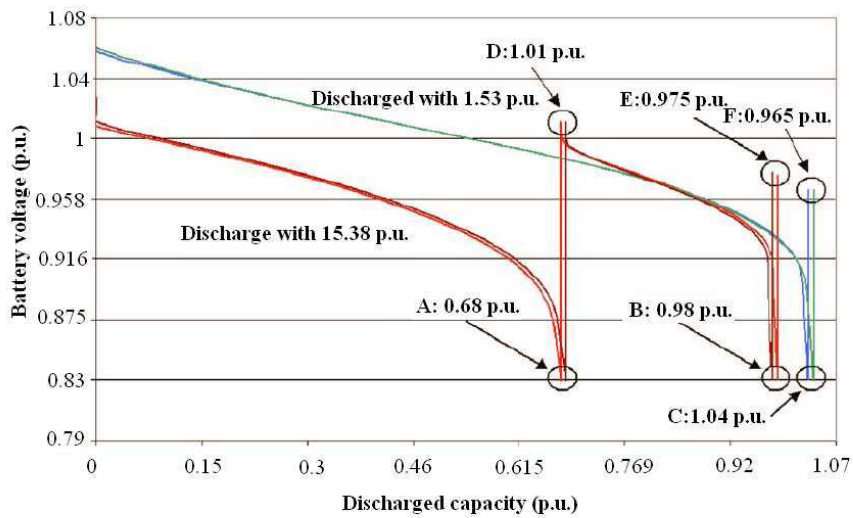
Base capacity	Base discharge time	Base current	Base voltage	Base power	Base impedance
65 A·h	20 h	3.25 A	12 V	39 W	3.69 Ω

Table 5.8: Base values for the BLA1 battery used by Doerffel

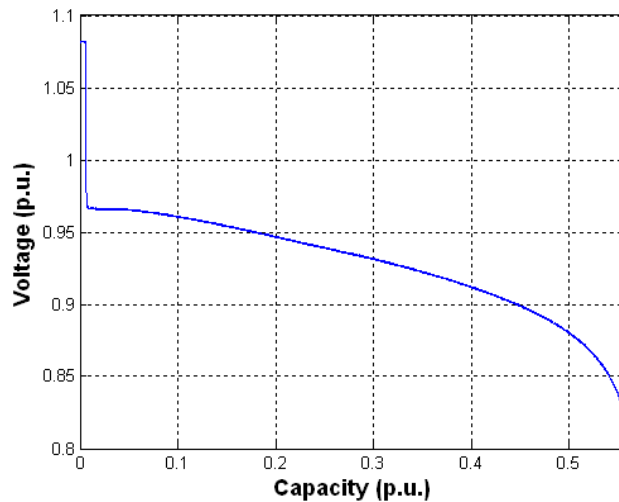
Comparing these two figures, there is apparently no relationship between them, as e.g., the discharged capacity and current are different, as Doerffel discharges its battery at 50 A and the Exide-Tudor battery is discharged at 138.42 A. However, if a per-unit system is defined and the same curves are compared in per unit values, other conclusions may be extracted. For both cases a set of base values are presented in Tables 5.7 and 5.8.

For these base values the same curves can be depicted as in Fig. 5.24, in which a simple comparison can be made. If the absolute value of both discharge currents are expressed as per-unit values, both batteries are then discharged with a 15.38 p.u. current. With the same per-unit current the Exide-Tudor battery presents a higher activation voltage drop, which is the voltage drop present at the beginning of the discharge. However, the Exide-Tudor discharges an 18 % less capacity than the battery of Doerffel, even though the battery used by Doerffel has nearly 31 % more rated capacity.

For example, the battery tested by Doerffel has a discharged capacity of 44.2 Ah, but this value does not give any information about the remaining capacity without an explicit reference to the rated capacity of the battery. On the other hand, 0.68 p.u. as the discharge capacity contains all the necessary information, as it is already referred to the rated capacity, once the set of base values are stated once and for all. Expressing all the results as p.u. values has an added value, as it allows a simple and direct comparison with similar work carried out by different authors, with different batteries, which can have very different characteristics (rated capacity, open circuit voltage, discharge time, etc).



a)



b)

Fig. 5.24: Discharge curve obtained by a)Doerffel and b)Gauchia in p.u. values

5.6.3. Per-unit approach during alternate loads

The per-unit model and base magnitudes obtained in the previous section are especially useful for the interaction of the battery with other power systems also expressed in per-unit values. However, the dynamic behavior and internal processes of the battery include phenomena whose time horizon can be shorter than the 5 hours base time obtained previously. Hence, a more appropriate base system can be obtained to represent, study and compare

the internal electrochemical dynamic behavior of the battery.

This second temporal horizon is straightforward after conducting the EIS tests, as the most relevant phenomena takes place between 0.1 Hz and 6 kHz. For this frequency interval, the corresponding time range is 10 s and 0.16 ms, which is between three and seven orders of magnitude smaller than the 5 h discharge time horizon.

The dynamic time horizon is related to the frequency at which the dynamic processes occur. So a base frequency can be defined as a new base variable, which was not included in the previous base values due to the fact that these were defined for stationary values. However, the internal behavior of the battery is clearly dependant on the frequency, as reflected by the Nyquist plot. Hence, a criterion for the selection of the base frequency should be established. Studying the Nyquist plot, there are three singular candidate points to be considered. The first and second one are the cut-off frequencies for R_1C_1 and R_2C_2 , defined as:

$$f_{c1} = \frac{1}{R_1C_1} \quad f_{c2} = \frac{1}{R_2C_2} \quad (5.8)$$

The third possible point is the resonance frequency, defined as the frequency at which the capacitive and inductive impedances cancel each other, and therefore the battery impedance becomes purely resistive:

$$Z_{total}(\omega) = \left[R_{ohm} + \frac{R_1}{1 + \omega^2 C_1^2 R_1^2} + \frac{R_2}{1 + \omega^2 C_2^2 R_2^2} \right] + \dots \quad (5.9)$$

$$\dots + j\omega \cdot \left[L - \frac{C_1 R_1^2}{1 + \omega^2 C_1^2 R_1^2} - \frac{C_2 R_2^2}{1 + \omega^2 C_2^2 R_2^2} \right]$$

$$\text{Re}[Z(\omega)]_{\omega=\omega_r} = R_{ohm} + \frac{R_1}{1 + (2\pi f_r)^2 C_1^2 R_1^2} + \frac{R_2}{1 + (2\pi f_r)^2 C_2^2 R_2^2} \quad (5.10)$$

The choice of the resonance frequency as the base frequency has a relevant advantage compared to the cut-off frequency, which is the simple identification in the Nyquist plot where $\text{Im}[Z(\omega)] = 0$, or in the Bode plot, where $\omega = 0$. As seen in Fig. 5.8, the resonance frequency is variable, as it decreases with increasing state of charge; therefore, one point of the curve must be selected as base frequency. Considering that the rest of base magnitudes

were selected for rated values and fully charged battery, it is logical to infer that the base frequency should also be selected for a fully charged battery. Therefore, the base frequency chosen for our Exide-Tudor battery is 189.87 Hz.

Known this base frequency, the frequencies magnitudes can be expressed in per-unit values for the rest of points of the EIS tests, if e.g. one point is at 400 Hz, its per-unit frequency would be 2.01 p.u. As it happened with the rest of per-unit magnitudes, knowing the per-unit frequency reveals more information than the absolute frequency. 2.01 p.u. means that the battery behavior is inductive, as the per-unit frequency is larger than 1 p.u., whilst 400 Hz does not give this information.

5.7. Conclusions

EIS tests were also applied to model the dynamic nonlinear behavior of batteries. A high number of tests were necessary due to the fact that batteries can present a wide range of states of charge, as well as accept an also wide range of currents. For both situations, charge and discharge processes were tested. However, time domain tests were also necessary to obtain the open circuit voltage hysteresis effect. This effect is rarely taken into account but can affect the resulting accuracy of model.

The direct comparison in absolute values of the equivalent circuit parameters renders confusing results due to the disparity of voltages and capacities. Therefore, in this Thesis we propose a per-unit system to correctly carry out this comparison, which, up to now, has not been found in literature. The per-unit system proposed includes, apart from the classical base voltage, current, power and impedance, a base time. Time is a key variable in batteries, due to the limited amount of reactants contained in the battery casing, and is related to capacity and current.

Batteries, as fuel cells, generate dc power. However, they can also accept, up to some extent, a certain amount of ac component superimposed on the dc current load. This ac current load frequency will influence the battery impedance behavior, and should therefore be taken into account. Through

the EIS tests carried out it is possible to know the capacitive, resistive and inductive behavior of the battery impedance. Therefore, for these ac component it is possible to define a base frequency. Various points were considered as possible base frequencies, but finally the resonance frequency was chosen. This choice was due to the resistive behavior at the resonance point (1 p.u.), which clearly identifies any capacitive (smaller than 1 p.u.) or inductive behavior (larger than 1 p.u.). Moreover, it is an easily identifiable point in both the Nyquist and Bode plots.

Nonlinear dynamic model for ultracapacitors

6.1. Introduction

This chapter presents a nonlinear dynamic model of ultracapacitors (also called supercapacitors) for simulation purposes. The model is experimentally validated under abrupt current loads.

The ultracapacitor modeled is a 3000 F 2.5 V Maxwell Boostcap. Its principal characteristics and photograph are shown in Table 6.1 and Fig. 6.1.

6.2. EIS tests experimental procedure

Ultracapacitors are receiving great attention by researchers, and due to its more recent development, the modeling techniques and model topology are still under investigation, as presented in the State-of-the-art, and there is not an unanimous equivalent circuit topology.

Capacitance	C (F)	3000
Maximum voltage	U (V)	2.7
DC series resistance	ESR dc ($m\Omega$)	0.29
Series resistance at 1 kHz	ESR 1kHz ($m\Omega$)	0.24
Leakage current	Ic (mA)	5.2
Shortcircuit current	Isc (A)	4800
Maximum specific energy	E _{max} (Wh/kg)	5.52
Maximum specific power	P _{max} (W/kg)	13.8
Weight	m (kg)	0.55

Table 6.1: Maxwell Boostcap 3000F ultracapacitor characteristics



Fig. 6.1: 3000F Maxwell ultracapacitor

Moreover, ultracapacitors are high power elements, which are capable of working with very high currents (hundreds of amperes) and which need special test conditions, which require equipments able to manage very high currents and small voltages.

Normally, impedance analyzers accept low currents (e.g. 60 mA) and medium voltages (45 V). This low maximum current forces the use of other equipments along with the impedance analyzer, such as potentiostats, which are able to absorb higher dc currents. Some examples are the 1287 A Solartron potentiostat, which endures up to 2 A, the Multi-Channel Cell Test System, also by Solartron, with a 5 A limit or the HCP-1005 Kromatec potentiostat which includes an 100 A booster.

The EIS tests can be carried out either with current control (galvanostatic mode) or with voltage control (potentiostatic mode). Either option requires an ac power source able to operate in a wide range of frequencies, at very high currents and low voltages. These conditions are very difficult to find in

conventional equipments (either potentiostats or power sources).

The current range is determined by the element under study. For very large capacitance values, such as those used in this work (3000 F 2.5 V) it can be easily deduced that current variations are as large as hundreds of amperes, which result in voltage variations of only some mV, the minimum value required to have a good signal-to-noise ratio. To carry out EIS tests under these conditions, the available commercial equipments were not useful. Therefore, in this Thesis we propose an experimental setup which allows to conduct frequency and time domain tests with high currents in a flexible and low cost way.

6.2.1. EIS test conditions

The first important decision which must be taken is under which mode the EIS tests should be carried out: galvanostatic or potentiostatic. To apply a potentiostatic (voltage control) EIS test it is necessary to use an ac power source, able to absorb high currents with low voltage and be able to work in a very wide range of frequencies. It is difficult to find an equipment which fulfills all these requirements. Therefore, the EIS tests are conducted in galvanostatic mode. Even if current is the control variable, the ultracapacitor voltage must be carefully monitored, to avoid over-voltage.

In order to define the range of current amplitudes to be used during the EIS tests, a series of previous measurements were made, starting at 20 A. In all cases the resulting voltage amplitudes were measured. It was found that, due to the very large capacitance of the ultracapacitor, the EIS results for ac currents below to 150 A were useless due to the insufficient ac voltage amplitude, which caused an incorrect impedance calculation. At 150 A, the EIS tests results were clear enough to ensure a correct measure, with an ac voltage amplitude of 70 mV.

The ac signal frequency is variable between 0.1 Hz and 1 kHz. The lower frequency limit is chosen due to the fact that smaller frequencies would lengthen the test duration and cause a significant variation of the test conditions.

The maximum frequency is limited to 1 kHz because the ultracapacitor inductive behavior is already clearly identified at this frequency.

For other electrochemical systems, such as batteries or fuel cells, the ac component is normally superimposed to a dc level. However, ultracapacitors charge and discharge very quickly and it is difficult to keep the test conditions in a narrow interval. For example, the discharge time can be as short as 30 s, with a voltage variation from 2.7 rated voltage to 0 V. EIS tests, taking into account the frequency range lasts 15 minutes, so an EIS tests during a dc discharge is not possible. Moreover, the tests conditions should be kept as constant and invariable as possible, so a variation of the 100% of the test voltage is unacceptable. Therefore, the ac current will be the only current absorbed/supplied by the ultracapacitor. This test procedure guarantees that the voltage at the beginning and end of the test will be the same due to the fact that the energy stored during half of the period of the ac current signal will be discharged during the other half. The authors who have applied EIS to ultracapacitors did it in potentiostatic mode (voltage control). Only Buller [18] carried out a galvanostatic mode EIS, but did not describe the test procedure.

In order to obtain an equivalent circuit, the dependency of the parameters of the equivalent model with current and/or voltage should be investigated. As explained in [21], [20] or [17], and unlike batteries or fuel cells, ultracapacitors parameters depend on the voltage, instead of the current, so the charge stored depends on the capacitance and voltage.

Taking into account the preceding considerations, the ultracapacitor will be tested under the following conditions:

- DC current: 0 A.
- AC current amplitude: 150 A.
- DC voltage: 1.5 V, 2 V and 2.5 V.
- Frequency: 0.1 Hz to 1 kHz.

6.2.2. EIS experimental setup proposed

To carry out the EIS tests, the equipment used is the following:

- Impedance analyzer: Solartron 1260.
- DC Electronic load: Chroma 63201 (60 V, 300 A).
- DC Power source: Sorensen 20-150E (12 V, 150 A).
- dSpace PX 10. The signals are acquired through an input/output board DS 2201, which is connected to its connector panel CP 2201. Both elements are part of a dSpace real-time control and acquisition system. The I/O DS 2201 board has 20 input channels, with 5 A/D converters which multiplex 4 channels each. There are 8 output channels with 8 parallel D/A converters. All the channels have a 12 bit resolution.
- LEM transducer: LA-205 S.
- Computer.

The EIS test is controlled by the impedance analyzer, which is the equipment which varies the frequency and monitors current and voltage to calculate the impedance. Due to the fact that it cannot directly generate a 150 A ac signal, the impedance analyzer controls other equipments which can work at high currents: the dc electronic load and power source. As explained in Figs. 6.2 and 6.3, the impedance analyzer is programmed to generate an ac voltage signal, which is monitored by the dSpace system. Through Matlab/Simulink, this signal is separated in its positive and negative semi-cycles. The positive semi-cycle is scaled to control the electronic load, which will sink the corresponding ac current. Meanwhile, the negative semi-cycle is scaled to program the dc power source, which will supply the corresponding ac current. Therefore, the coordinated and real-time control of the electronic load and power source results in a constant amplitude/variable frequency current at the ultracapacitor terminals, which follows the control signal generated by the impedance analyzer.

According to the wiring diagram depicted in Fig. 6.4, the ultracapacitor is connected in parallel to the electronic load and power source. In this way, it can absorb the current during positive semi-cycles and release it during

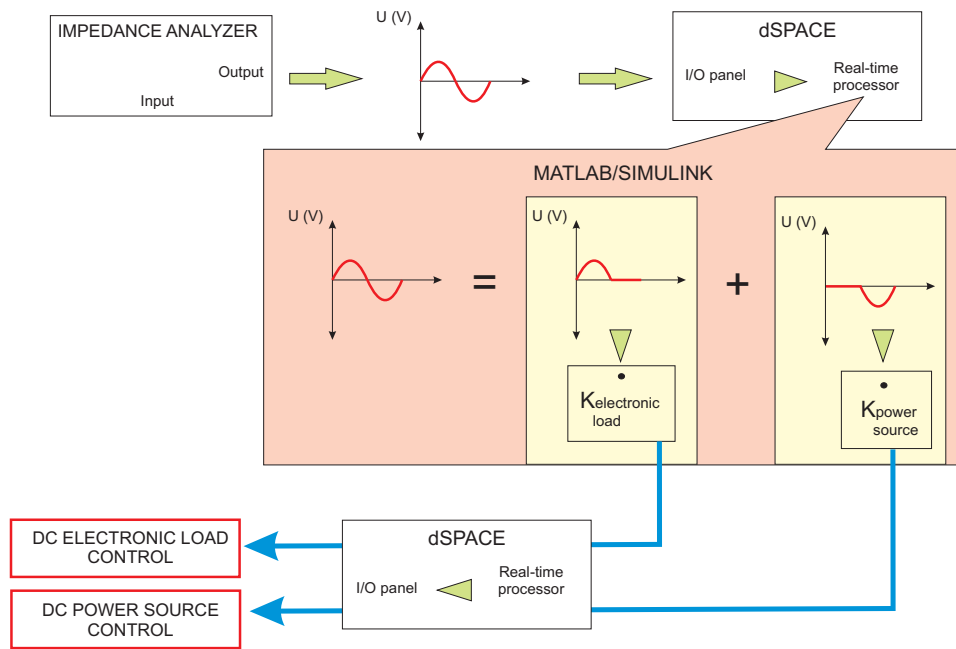


Fig. 6.2: EIS control procedure for ultracapacitors

negative semi-cycles. A current LEM transducer is connected in series with the ultracapacitor to measure the current, which is sent to the impedance analyzer. The voltage at terminals of the ultracapacitor is directly sent to the impedance analyzer, which accepts dc voltages smaller to 42 V. With the current and voltage measures the impedance analyzer is able to calculate the ultracapacitor complex impedance. The laboratory setup diagram and photograph are shown in Figs. 6.4 and 6.5.

6.2.3. EIS tests results

The graphical representation of the EIS tests are the Nyquist plots shown in Fig. 6.6. The ultracapacitor capacitive behavior is restricted to a small interval (from 0.1 Hz to 31.6 Hz). For the lower frequencies of this interval the Nyquist plot is practically a vertical line, which is the representation of a capacitance in series with a resistance, whose value ($0.25 \text{ m}\Omega$) is identified as the intersection between the curve and the abscissa axis. In literature, this part of the curve is not totally vertical due to the contact resistance between components, high electrode porosity or low proton mobility inside the electrodes [95].

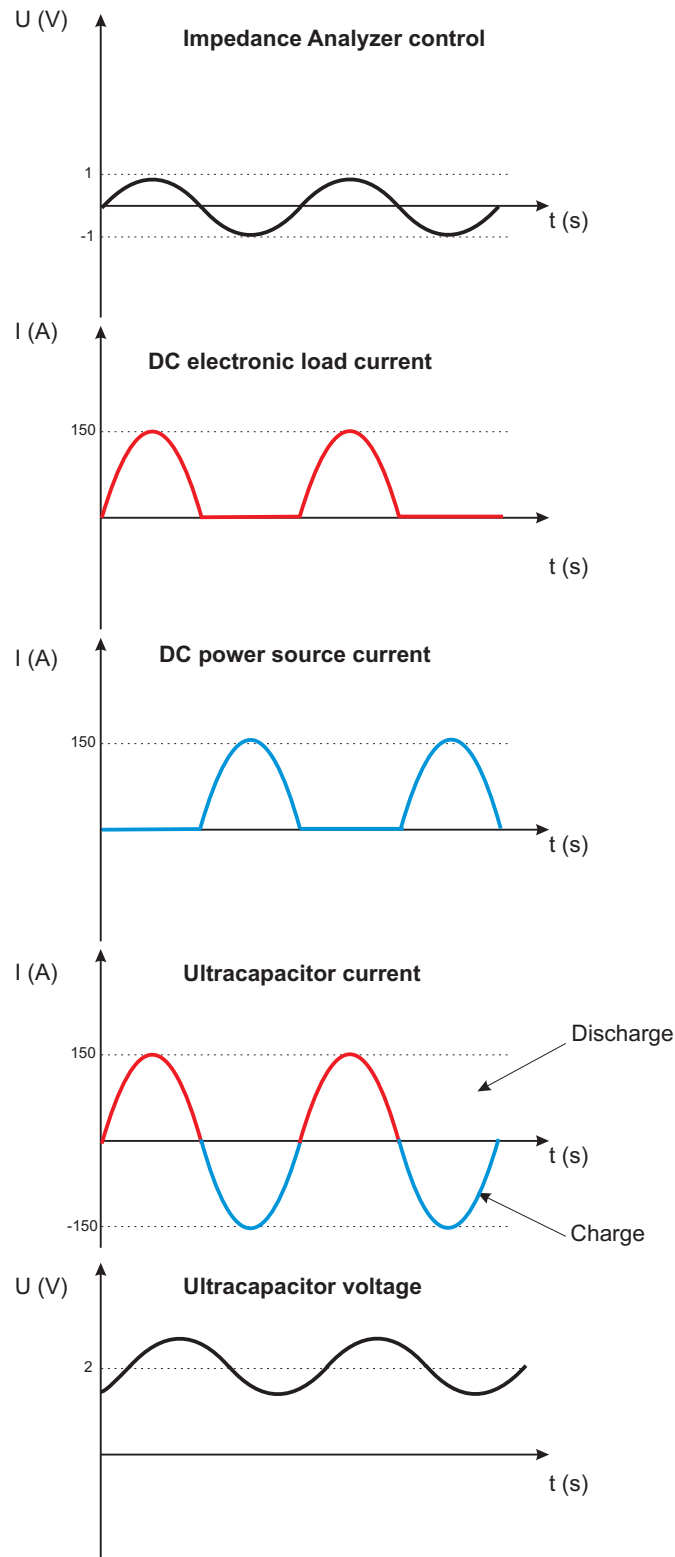


Fig. 6.3: Currents and voltage evolutions for each equipment

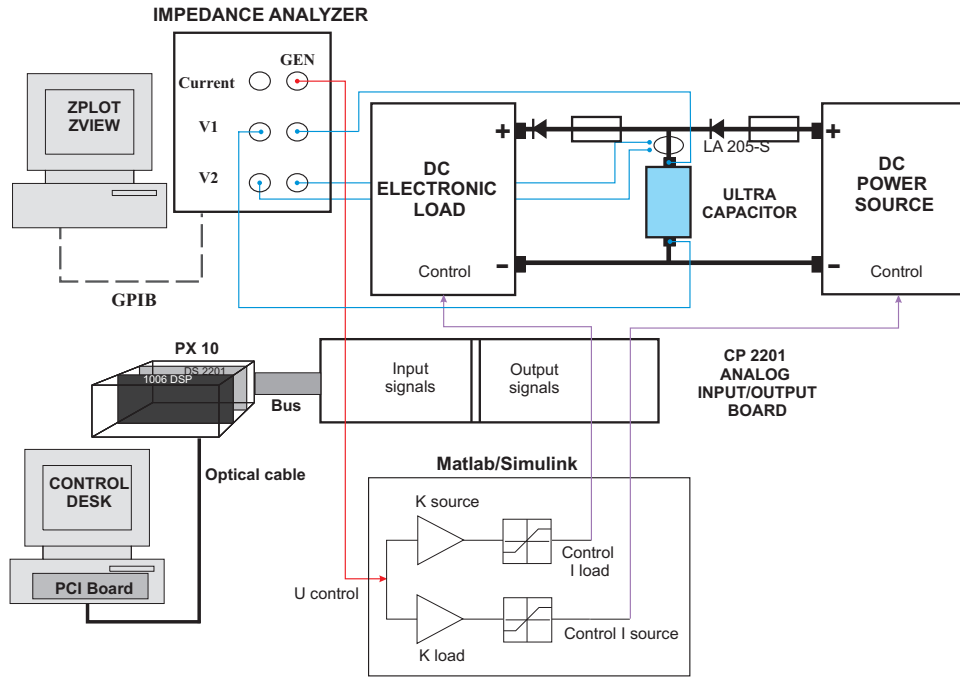


Fig. 6.4: EIS experimental setup

From 1 Hz to 31.6 Hz the complex impedance changes to a 45° slope due to diffusion phenomena at the electrode pores. In literature, some authors such as Barsoukov [46] and Brouji [76] explain that the ultracapacitor electrodes are highly porous structures, through which the charge transport resembles a transmission power electric line, due to the fact that the pore diameter is small compared to its length. This diffusion phenomena can be represented by a Warburg impedance, which is the series connection of RC networks. In this Thesis, the diffusion has been represented with two RC networks, avoiding the use of higher number of networks, which complicate the modeling and require more computational work.

From 31.6 Hz onwards, the ultracapacitor behavior is totally inductive. In literature, most authors neglect or do not comment the ultracapacitor inductive behavior and do not present this region on the Nyquist plot. Other authors such as [18], just mentions it, whilst [21] or [20] state that during inductive behavior the real part of the impedance increases due to skin effect. However, our results show that the real part of the impedance decreases before it starts increasing. At these frequencies, the current does not flow

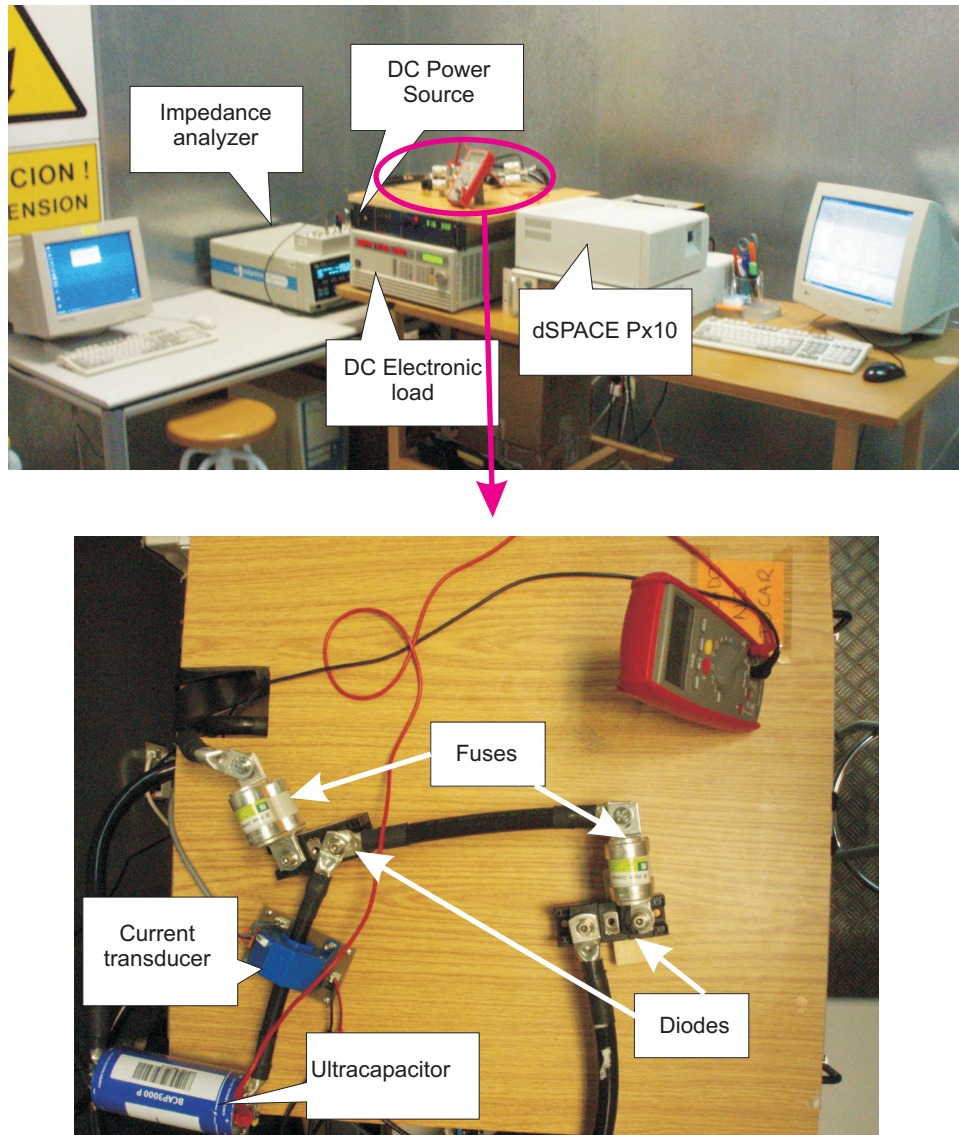


Fig. 6.5: Photograph of the ultracapacitor EIS setup

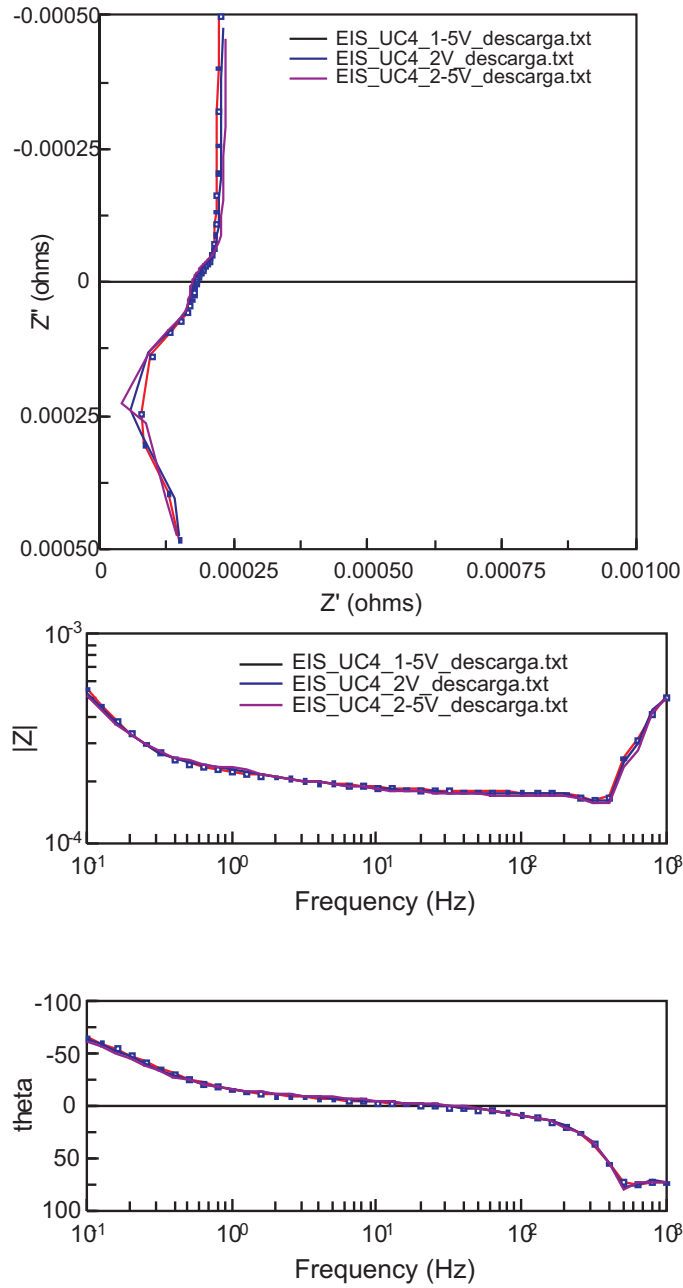


Fig. 6.6: Nyquist and Bode plots obtained for the ultracapacitor after the EIS tests

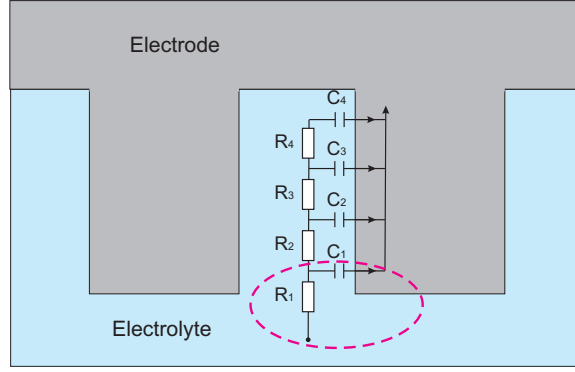


Fig. 6.7: High frequency effect on the pore effective surface. Adapted from [29]

inside the pores, but stays at the beginning of the pore, as depicted in Fig. 6.7. This implies that most of the current flows through the bulk material, whose resistance is smaller than the electrolyte resistance, causing the reduction seen in the Nyquist plot. When the frequency increases this effect is summed up with the skin effect, which causes an eventual increase of the real part of the impedance. The real part of the impedance should be always positive, therefore, possible negative values are due to small errors present when the real part of the resistance is $10^{-4} \Omega$.

Among the wide variety of equivalent circuits under study, the best fit of the Nyquist plot was found for the circuit structure shown in Fig. 6.8. The parameters obtained present assumable errors, and only one parameter presents an error bigger than 10%. The values obtained from ZView were introduced in the software Statgraphics, in order to obtain the polynomial dependency of each parameter with the voltage. The model obtained explains the 100% of the variability. The equations obtained are shown in (6.1).

$$\begin{aligned}
 L \text{ (H)} &= 1.15 \cdot 10^{-7} - 7.10 \cdot 10^{-9} \cdot U + 8.80 \cdot 10^{-10} \cdot U^2 \\
 C_1 \text{ (F)} &= 1816 + 1260 \cdot U - 244 \cdot U^2 \\
 C_2 \text{ (F)} &= 2307 - 648 \cdot U + 100 \cdot U^2 \\
 R_2 \text{ (\Omega)} &= 1,16 \cdot 10^{-5} + 2,09 \cdot 10^{-5} \cdot U - 0,19 \cdot 10^{-5} \cdot U^2 \\
 C_3 \text{ (F)} &= 1.51 + 1.11 \cdot U - 0.29 \cdot U^2 \\
 R_3 \text{ (\Omega)} &= 6,39 \cdot 10^{-4} - 1,47 \cdot 10^{-4} \cdot U + 0,36 \cdot 10^{-4} \cdot U^2
 \end{aligned} \tag{6.1}$$



Element	Freedom	Value	Error	Error %
L1	Free(+)	1,0728E-7	1,5885E-9	1,4807
C1	Free(+)	3157	75,692	2,3976
C2	Free(+)	1560	319,51	20,481
R2	Free(+)	3,8784E-5	3,9544E-6	10,196
C3	Free(+)	2,532	0,099294	3,9216
R3	Free(+)	0,00016681	2,193E-6	1,3147

Chi-Squared: 0,01661
 Weighted Sum of Squares: 1,2624

Data File: D:\SANDRA\RESULTADOS EIS UC\Definitivos\EIS t
 Circuit Model File: D:\SANDRA\RESULTADOS EIS UC\Circuito Equival
 Mode: Run Fitting / Freq. Range (0,1 - 1000)
 Maximum Iterations: 800
 Optimization Iterations: 0
 Type of Fitting: Complex
 Type of Weighting: Calc-Modulus

Fig. 6.8: Equivalent circuit fitted with ZView

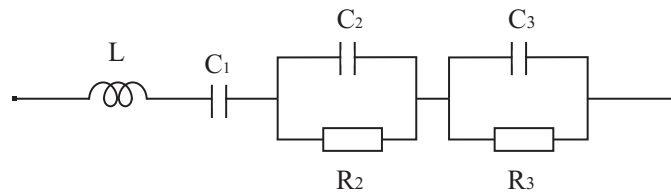


Fig. 6.9: Ultracapacitor equivalent circuit

6.2.4. Ultracapacitor impedance model and validation

With the previous equations, the model obtained is shown in Fig. 6.9. It can be observed that, unlike batteries or fuel cells, the ultracapacitor model is a purely passive model, with no voltage or current sources. All the elements involved present electrical equations, which are easily programmed in Matlab/Simulink. The voltage at the ultracapacitors terminal programmed corresponds to 6.2.

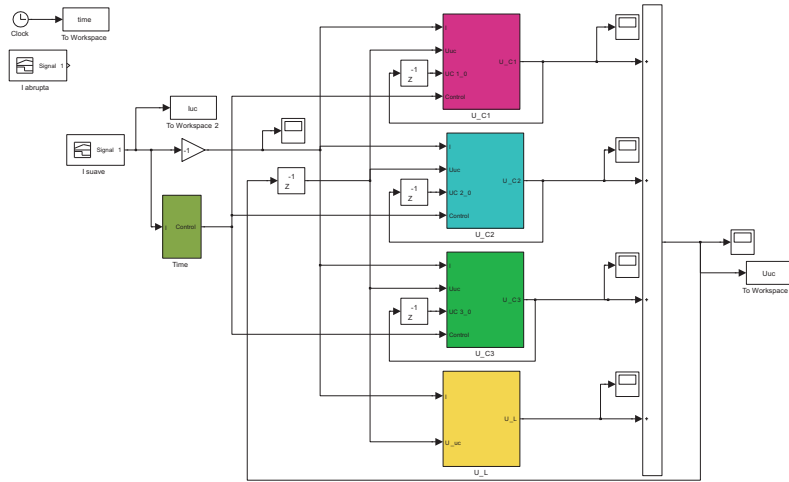


Fig. 6.10: Ultracapacitor Matlab/Simulink model

$$\begin{aligned}
 U_{uc} &= U_L + U_{C_1} + U_{C_2} + U_{C_3} \\
 U_L &= L \cdot \frac{dI}{dt} \\
 U_{C_1} &= \int \frac{1}{C_1} \cdot I \cdot dt \\
 U_{C_2} &= \int \frac{1}{C_2} \cdot \left(I - \frac{U_{C_2}}{R_2} \right) \cdot dt \\
 U_{C_3} &= \int \frac{1}{C_3} \cdot \left(I - \frac{U_{C_3}}{R_3} \right) \cdot dt
 \end{aligned} \tag{6.2}$$

The ultracapacitor model has two inputs and one output. The inputs are the current demanded and the voltage at its terminals. This ultracapacitor model needs an initial voltage value to begin the simulation. The model output is the voltage at the terminals of the ultracapacitor. The Matlab/Simulink model is shown in Fig. 6.10

To obtain an experimental validation of the model, an abrupt load current profile, depicted in Fig. 6.11, was programmed and the voltage at terminals monitored. The experimental and modeled voltages are compared in Fig. 6.12. It can be observed that the ultracapacitor time constant is very small and causes the dynamic evolution to present a linear evolution under abrupt

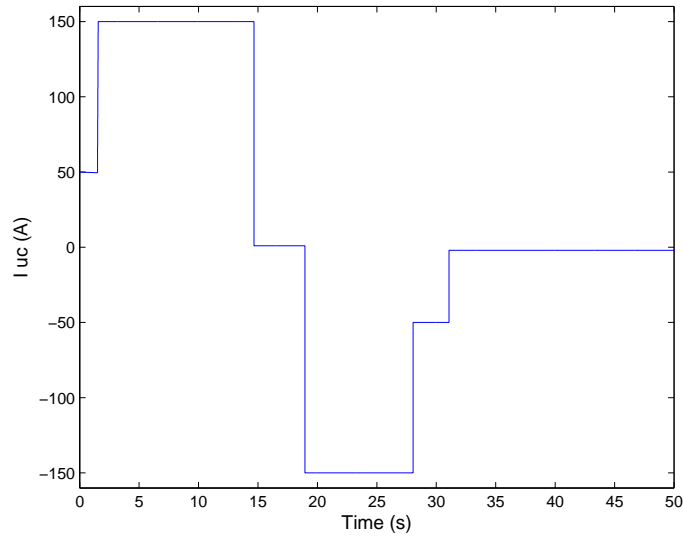


Fig. 6.11: Abrupt ultracapacitor current load

current profiles. The model follows quite precisely the experimental voltage.

6.3. Conclusions

Ultracapacitors are a relatively new technology, and therefore, its test procedure, equivalent circuit and characteristic curve are not universally defined. Moreover, ultracapacitors are high power elements which need special test considerations. These considerations are rarely mentioned in literature, where authors avoid disclosing its test setup and procedure, and most of them do not make any attempt to validate the model proposed.

Ultracapacitors tested up to now are usually smaller than the 3000 F ultracapacitor tested in this Thesis. Therefore, the equipments used by other authors, frequently not mentioned, are not applicable due to its small current limit. In this Thesis we propose an EIS test procedure which allows to carry out these test during the high currents needed to obtain a correct impedance calculation. The setup proposed uses conventional laboratory equipments, such as dc electronic load and dc power source, which can be synchronously controlled by an impedance analyzer through a real-time acquisition and control system.